Eur J Med Chem (1995) 30, 823–838

A reversible monoamine oxidase inhibitor, Toloxatone: comparison of its physicochemical properties with those of other inhibitors including Brofaromine, Harmine, R40519 and Moclobemide

F Moureau[1], J Wouters[1], M Depas[1], DP Vercauteren[2], F Durant[1], F Ducrey[3], JJ Koenig[3]*, FX Jarreau[3]

[1]*Laboratoire de chimie moléculaire structurale, Facultés universitaires Notre-Dame-de-la-Paix;*
[2]*Laboratoire de physicochimie informatique, Facultés universitaires Notre-Dame-de-la-Paix, 61, rue de Bruxelles, B-5000 Namur, Belgium;*
[3]*Synthélabo Recherche, Centre de Rueil, 10, rue des Carrières, 92500 Rueil-Malmaison, France*

(Received 14 February 1995; accepted 21 June 1995)

Summary — Reversible, competitive and selective monoamine oxidase A inhibitors (MAO_AIs) are an exciting new type of antidepressants with a safe profile. The mechanism for reversible inhibition of MAO_A at the molecular level is still unknown. The planar structure of most reversible MAO_AIs and the well-defined acceptor power of flavin adenine dinucleotide (FAD), the cofactor of the enzyme, suggest that MAO_AIs exert their inhibitory effect through charge-transfer interactions with the FAD. This hypothesis has been evaluated for Toloxatone **1**, the first reversible MAO_AI marketed in France. In this work, we give evidence for the ability of other reversible MAO_AIs, including Brofaromine **2**, Harmine **3** and R40519 **4** to interact with the flavin cofactor in comparison with Moclobemide **5**, and we underline the physicochemical properties required for these interactions. First, the formation of a complex between each of the MAO_AIs and riboflavin, a model of the flavin cofactor, is shown by electronic absorption spectroscopy. Essential electronic descriptors of MAO_AIs, such as the molecular electrostatic potential and the topology of the frontier orbitals, are then calculated by the *ab initio* Hartree–Fock method and compared with those of previously studied Toloxatone. This confirms the electronic absorption spectroscopy results. Finally, the similarities between the different MAO_AIs are underlined and an interaction model is discussed on the basis of a detailed analysis of the electronic descriptors of all the considered MAO_AIs and the flavin nucleus.

reversible MAO_AI / FAD / charge transfer / frontier orbital topology / molecular electrostatic potential / interaction model

Introduction

Depression is a very widespread mental disease in the adult population. The first antidepressant candidates for clinical testing appeared around the middle of this century in the form of monoamine oxidase inhibitors (MAOIs). Monoamine oxidase (MAO, EC 1.4.3.4) is a flavoenzyme located on the outer wall of mitochondria [1]. Two forms, MAO_A and MAO_B, have been identified on the basis of pharmacological, biochemical and immunological criteria (for a review see reference [2]). These two forms are composed of two identical subunits, both linked to the flavin adenine dinucleotide (FAD) [3] (fig 1). Although the peptide sequences of these two forms present certain differences, the cofactor FAD is linked covalently to the same pentapeptide (Ser-Gly-Gly-Cys-Tyr) [4].

Three generations of MAOIs have been successively described. The first generation includes the irreversible and non-selective inhibitors, and the second, the irreversible and selective ones. The third generation is constituted of MAOIs that have the advantage of acting through a reversible and selective mode, which are therefore an exciting new type of antidepressants with a safe profile compared with the previous MAOIs [5].

The mechanism of action at the molecular level of irreversible MAOIs of the two first generations has been extensively studied. They all act as mechanism-based inhibitors. First, they form a reversible complex with the FAD cofactor of the enzyme; they are then, by means of the same catalytic process as for substrates, transformed into intermediate oxidized

*Correspondence and reprints

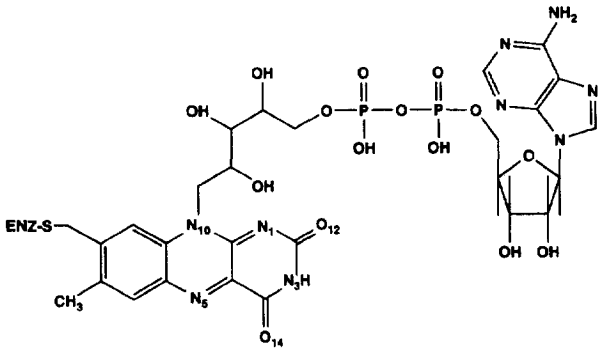

Fig 1. Planar structural formula of flavin adenine dinucleotide (ENZ = enzyme peptide chain).

species. Finally, these reactive species engage in covalent binding to the enzyme through an intermediate reduced form of FAD [6].

On the other hand, the mechanism of action for the reversible and selective MAOIs of the third generation is still unknown. A hypothesis has been proposed for MAO_BIs, which are mechanism-based inhibitors [7].

The purpose of this work is to study reversible non-substrate MAO_A inhibitors, Toloxatone **1**, in comparison with Brofaromine **2**, Harmine **3** and R40519 **4**, and also with Moclobemide **5**, a reversible but substrate-type inhibitor.

Aryl-2-oxazolidinones constitute an important family of reversible MAOIs synthesized by Synthélabo-Delalande Laboratories [8]. Stereoelectronic studies of these compounds and structure–activity relationships within this family led to the hypothesis of a physical association between the MAO_AIs and FAD, the cofactor of MAO_A [9]. This proposition was confirmed for Toloxatone **1**, 5-hydroxymethyl 3-tolyl oxazolidinone (fig 2), which was the first reversible MAO_AI marketed in France (Humoryl®) in 1985. Electronic absorption measurements demonstrated the existence of a charge-transfer complex with riboflavin, a model of the flavin cofactor, while *ab initio* Hartree–Fock calculations of frontier orbital topologies and molecular electrostatic potentials of the two partners confirmed the favourable overlap of complementary electronic regions for one well-defined relative orientation as detailed in a previous report [10].

The aim of this contribution is to confirm the potential of other reversible MAO_AIs to interact with FAD through weak reversible forces and consequently to underline the stereoelectronic properties required for this interaction. Four inhibitors were selected for this purpose: Brofaromine **2**, Harmine **3**, R40519 **4** and Moclobemide **5** (fig 2).

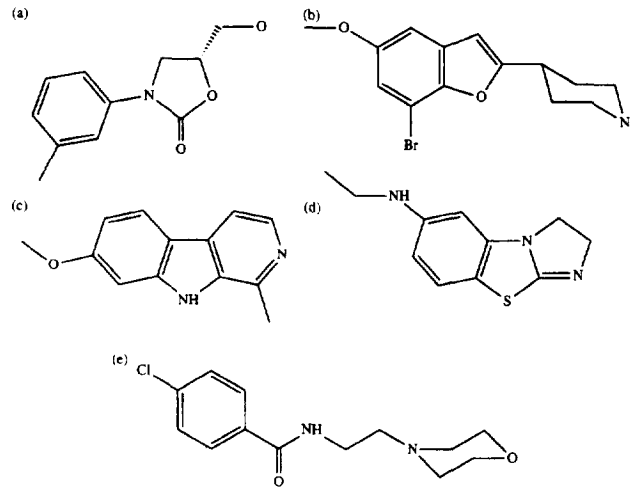

Fig 2. Structural formulae of (a) *R*-Toloxatone **1**, (b) Brofaromine **2**, (c) Harmine **3**, (d) R40519 **4**, and (e) Moclobemide **5**.

The first three compounds are highly potent and selective MAO_A inhibitors as determined by *in vitro* studies. Brofaromine **2**, 4-(5-methoxy-7-bromobenzofuranyl-2)piperidine, is a MAOI in development by Ciba-Geigy Laboratories (Basel, Switzerland); $IC_{50}A$ = 0.013 μM and $IC_{50}B$ = 31 μM [11]. Recent biological studies have clarified that Brofaromine is a tight-binding inhibitor [12]. Harmine **3**, 1-methyl-7-methoxy-β-carboline, is an alkaloid belonging to the Harmala family; $IC_{50}A$ = 0.003 μM and $IC_{50}B$ = 7 μM; K_iA = 0.004 μM [13, 14], *ie* more potent than its saturated analogues [15, 16]. R40519 **4**, *N*-ethyl-2,3-dihydroimidazo[2,1-*b*]benzothiazol-6-amine, was synthesized by Janssen Pharmaceutica Laboratories (Beerse, Belgium) but is rarely quoted in the scientific literature; $IC_{50}A$ = 0.050 μM and $IC_{50}B$ = 55 μM [17].

Moclobemide **5**, *p*-chloro-*N*-[2-morpholinoethyl]-benzamide was synthesized by Hoffmann–La Roche Laboratories (Basel, Switzerland) and is not a very potent MAO_AI: $IC_{50}A$ = 6.1 μM and $IC_{50}B$ > 1000 μM [11]. It displays a higher potency *in vivo* than predicted from the *in vitro* experiments [18]. To our knowledge, the mechanism of inhibition of Moclobemide has not yet been elucidated, but it should have some similarities with that proposed for irreversible MAOIs, except that the covalent binding could be broken by metabolization. Indeed, it is possible that it behaves as a mechanism-based, enzyme-activated inhibitor of MAO_A, undergoing conversion by the enzyme itself into an intermediate which inhibits the enzyme without prior release from the active site [19, 20].

This study is subdivided in three parts. First, the formation of a complex between each of the four MAO_AIs and riboflavin, used as a model for FAD, is analysed by electron absorption spectroscopy. Electronic parameters of the MAO_AIs, such as frontier orbital topologies and molecular electrostatic potentials, computed at the *ab initio* Hartree–Fock level, are then described and compared with those of Toloxatone as studied previously [10]. Finally, a model of the interaction is proposed.

Results and discussion

Electronic absorption spectroscopy

FAD, the cofactor of MAO, is an isoalloxazine derivative. In view of its well-known acceptor properties [21], we used by electronic absorption spectroscopy to analyze the formation of charge-transfer complexes between riboflavin used as a model of FAD and each of the four MAO_AIs selected.

When a donor D is mixed with an acceptor A, an equilibrium characterized by a complexation constant, K_C^{AD} is established between the complexed and the uncomplexed species.

The electronic absorption spectrum of such a solution corresponds to a modified spectrum of the two partners plus another absorption band, called 'extra' band. This band takes into account the intermolecular electron transfer and is always at a higher wavelength than the bands characteristic of the two molecules involved in the complex [22].

If (i) a complex of stoichiometry 1:1 only is formed between the acceptor and the donor; (ii) the formed complex absorbs only at a wavelength λ characteristic of the charge transfer; (iii) the initial donor concentration is greater than that of the acceptor; (iv) the Lambert–Beer law is respected; (v) the optical pathlength is 1 cm (for simplification in the mathematical expression); (vi) the maximum appears at a single wavelength value, all conditions (ionic strength, pH and temperature) being constant; and (vii) the solvent and buffer do not interact with either the donor or the acceptor, then the Foster–Hammick–Wardley equation can be evaluated as simply:

$$\frac{A}{[D]_0} = -K_C^{AD}A + K_C^{AD}[D]_0\varepsilon_\lambda^{AD} \qquad [1]$$

where $[D_0]$ is the initial concentration of the donor, *ie* the inhibitor, A is the absorbance at the wavelength λ_{max} characteristic of the complex, and ε_λ is the molar extinction coefficient of the complex in L mol^{-1} cm^{-1} [23]. Plotting $A/[D]_0$ *versus* A for several solutions of variable initial donor concentration and constant initial acceptor concentration gives a straight line, whose slope is equal, sign apart, to the complexation constant. Repeating this work at different temperatures and using the van't Hoff equation leads to the thermodynamic complexation parameters: ΔG^0, ΔH^0 and ΔS^0.

The electronic absorption spectra of solutions of constant riboflavin concentration with varying concentrations of Brofaromine, Harmine, R40519 or Moclobemide were recorded at four different temperatures. In order to optimize the visualization of the 'extra' band characteristic of the intermolecular transition, we used the difference spectra; the riboflavin spectrum was subtracted from the riboflavin/MAO_AI spectra. With the exception of Moclobemide, the difference spectra for the riboflavin/MAO_AI solutions (fig 3) are characteristic of charge-transfer complex spectra. Indeed, they reveal the existence of two absorption bands. The first at about 445 nm is characteristic of riboflavin and is of negative absorbance because the amount of non-complexed riboflavin in the sample cell is smaller than that in the reference cell and a certain amount of the riboflavin in the sample cell being complexed. The more negative the absorbance of this band, the greater the complexation. The second band of positive absorbance appears at different wavelengths according to the inhibitor: 492, 496 and 503 nm for Brofaromine, Harmine and R40519, respectively. This corresponds to the 'extra' band, characteristic of the intermolecular transition. The greater the absorbance of this band, the greater the concentration of complex in the solution. A charge-transfer band is usually broad, but in these cases, they are sharp, due to a negative overlap with

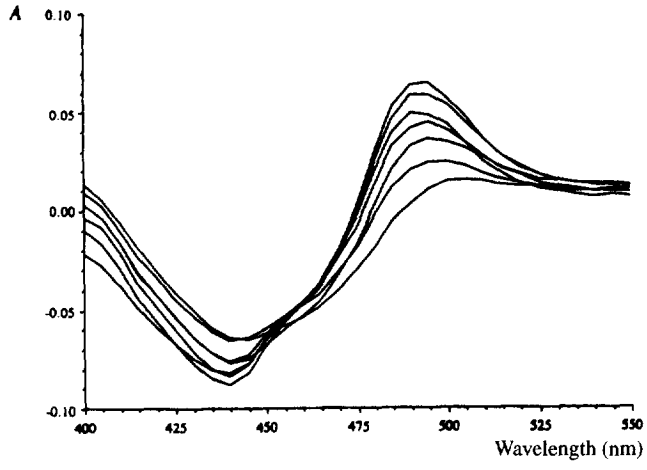

Fig 3. Difference absorption spectra of riboflavin/Brofaromine; concentration of riboflavin 1.00 x 10^{-4} M; 4.9 x 10^{-4} M ≤ [Brofaromine] ≤ 4.9 x 10^{-3} M; 11.0°C.

the band characteristic of riboflavin. The presence of isosbestic points confirms that complexes of stoichiometry 1:1 only are formed and that the Lambert–Beer law is respected.

The graph of $A/[D]_0$ as a function of A (fig 4), derived from the recorded spectra, demonstrates clearly that the Foster–Hammick–Wardley equations are fulfilled and corroborates the formation of complexes of 1:1 stoichiometry between riboflavin and Brofaromine. The same results were obtained for Harmine and R40519. This allows the determination of complexation constant, K_C^{AD}. The graph of ln K_C^{AD} as a function of $1/T$ (fig 5), corresponding to the van't Hoff equation, leads to the determination of the thermodynamic complexation parameters: ΔG^0, ΔH^0 and ΔS^0. The thermodynamic complexation parameters obtained for the riboflavin/Brofaromine, riboflavin/Harmine and riboflavin/R40519 complexes as well as the complex riboflavin/*R*-Toloxatone studied previously [10] are grouped together in tables I and II.

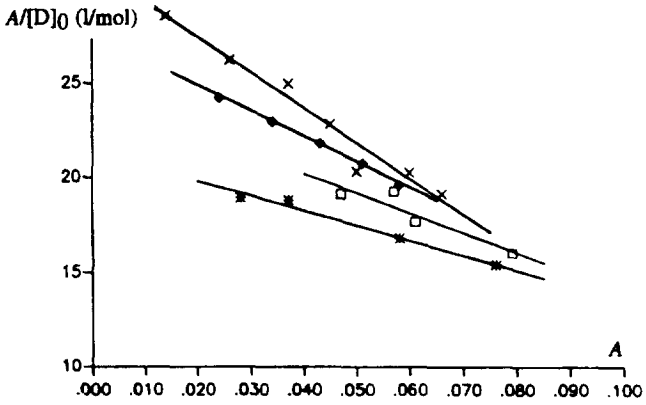

Fig 4. Plot of $A/[D]_0$ *versus* A for the riboflavin/Brofaromine molecular complexes. * 30.0°C; □ 22.0°C; ◆ 17.0°C; x 11.0°C.

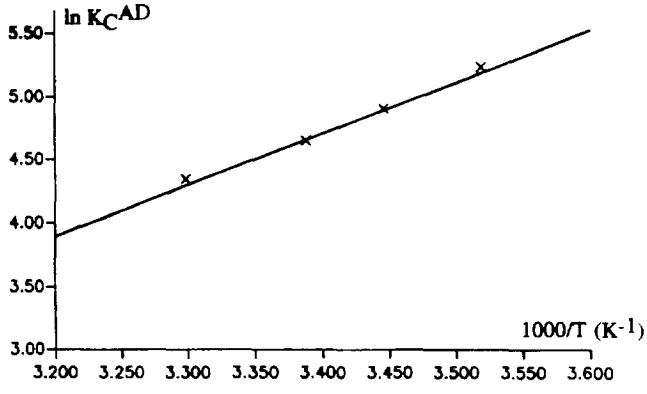

Fig 5. Plots of $\ln K_C^{AD}$ *versus* $1/T$ for the riboflavin/Brofaromine molecular complexes.

Similar spectrophotometric studies on riboflavin and FAD with amino acids, MAO substrates and MAO inhibitors of β-carboline type have previously been undertaken by Codoner *et al* [24–27]. The K_C^{AD}, ΔG^0, ΔH^0 and ΔS^0 parameters determined by these authors for the riboflavin/Harmine molecular complex are of the same order of magnitude as ours but are not identical (tables I and II). It is important to note that the thermodynamic complexation parameters must be considered with some caution because of the proximity of the charge-transfer band of the complex and the absorption band of riboflavin (see criterion (ii) above) which complicates the exact determination of λ_{max} as well as the absorbance measured at this wavelength. In spite of this, these parameters can be correlated to the affinity parameter K_iA, the wavelength characteristic of the intermolecular transition λ_{max}, and to the energy of the highest occupied molecular orbital E_{HOMO} (see next section) of the inhibitors (table III).

Table I. Equilibrium constants for the riboflavin/*R*-Toloxatone, riboflavin/Brofaromine, riboflavin/Harmine and riboflavin/R40519 molecular complexes (absorption spectroscopy data).

Compound	λ_{max} *(nm)*	K_C^{AD} *(L mol^{-1})*
R-Toloxatone	487	
0.0°C		107 ± 23[a]
5.5°C		88 ± 8[a]
10.0°C		81 ± 6[a]
Brofaromine	492	
11.0°C		188 ± 17
17.0°C		135 ± 4
22.0°C		105 ± 30
30.0°C		77 ± 8
Harmine	496	
5.0°		1400 ± 95[b]
9.5°C		1074 ± 97
15.0°C		1057 ± 58[b]
23.5°C		946 ± 93
27.0°C		735 ± 17[b]
34.6°C		619 ± 48
44.6°C		452 ± 37
45.0°C		411 ± 16[b]
R40519	503	
10.0°C		122 ± 6
20.5°C		111 ± 19
31.4°C		96 ± 29
40.2°C		88 ± 29

[a]Moureau [10]; [b]Codoner [27].

Table II. Thermodynamic parameters for the riboflavin/*R*-Toloxatone, riboflavin/Brofaromine, riboflavin/Harmine and riboflavin/R40519 molecular complexes (absorption spectroscopy data).

Compound	*ΔG^0 (0°C) (kJ mol^{-1})*	*ΔH^0 (kJ mol^{-1})*	*ΔS^0 (J K^{-1} mol^{-1})*
R-Toloxatone	− 10.6[a]	− 18.1[a]	− 27.4[a]
Brofaromine	− 13.1	− 33.8	− 75.7
Harmine	− 16.4[b] − 16.8	− 22.6[b] − 18.8	− 20.9[b] − 7.5
R40519	− 11.3	− 8.1	11.6

[a]Moureau [10]; [b]Codoner [27].

Table III. Inhibition constants (K_iA), wavelengths of the intermolecular transition band (λ_{max}), energies of the highest occupied molecular orbital (E_{HOMO}) and thermodynamic parameters of complexation (ΔG^0, ΔH^0 and ΔS^0) of riboflavin with Harmine, Brofaromine, R40519, *R*-Toloxatone and Moclobemide.

	Harmine	*Brofaromine*	*R40519*	*R-Toloxatone*	*Moclobemide*
K_iA (μM)	0.004[b]	0.006[c]	0.013[d]	1.5[a]	2.7[c]
λ_{max} (nm)	496	492	503	487[a]	485
E_{HOMO} (au)	− 0.21789	− 0.23526	− 0.17655	− 0.23545[a]	−
ΔG^0 (0°C) (kJ mol^{-1})	− 16.8	− 13.1	− 11.3	− 10.6[a]	−
ΔH^0 (kJ mol^{-1})	− 18.8	− 33.8	− 8.1	− 18.1[a]	−
ΔS^0 (J K mol^{-1})	− 7.5	− 75.7	11.6	− 27.4[a]	−

[a]Moureau [10]; [b]Nelson [13]; [c]value estimated according to the IC_{50} value determined by Da Prada [11]; [d]value estimated according to the IC_{50} value determined by van der Brempt [16].

The complexation between riboflavin and Harmine, Brofaromine, R40519 or *R*-Toloxatone induces a decrease in free energy: 16.8, 13.1, 11.3 and 10.6 kJ mol^{-1}, respectively. The greater the decrease, the more stable the complex and the higher the affinity of the considered inhibitor for the MAO_A (K_iA smaller).

Moreover, the wavelength λ_{max} characteristic of the complexes is closely correlated ($r = 0.95$) to the E_{HOMO} of the donors, *ie* the inhibitors. The higher the E_{HOMO}, the weaker the energy necessary for the electron transfer and thus the higher the λ_{max}. However, there is no correlation between either λ_{max} and the complexation ΔG^0 or E_{HOMO} and ΔG^0. This observation is not surprising. The charge-transfer component is not necessarily the dominating factor of the complex stability. Other additional interactions such as dipole interactions and dispersion forces can, in some cases, constitute the principal mode of binding.

As regards Moclobemide, the analysis of the results is more complicated. Under ambient light, the riboflavin/Moclobemide solution rapidly changes colour. It turns from intense yellow to orange-red and finally, after a few days, to pale yellow. The difference spectra recorded just after solution formation, after 1 d and after 12 d of exposure to light (fig 6) underline the colour changes. Apparently, Moclobemide first forms a charge-transfer complex with riboflavin which is characterized by a new absorption band at about 485 nm (fig 6a). After that, in contrast to the other three MAO_AIs, an additional phenomenon is shown by another colour change (intense yellow → orange-red) and the simultaneous appearance of a more intense absorption band at about 510 nm (fig 6b). This band could be attributed to an intramolecular transition within a newly formed chemical entity. This entity disappears rapidly as shown in figure 6c.

This succession of photochemical reactions could explain the particular biochemical profile of Moclobemide. Nevertheless, such an interpretation should be treated with caution because the photochemical

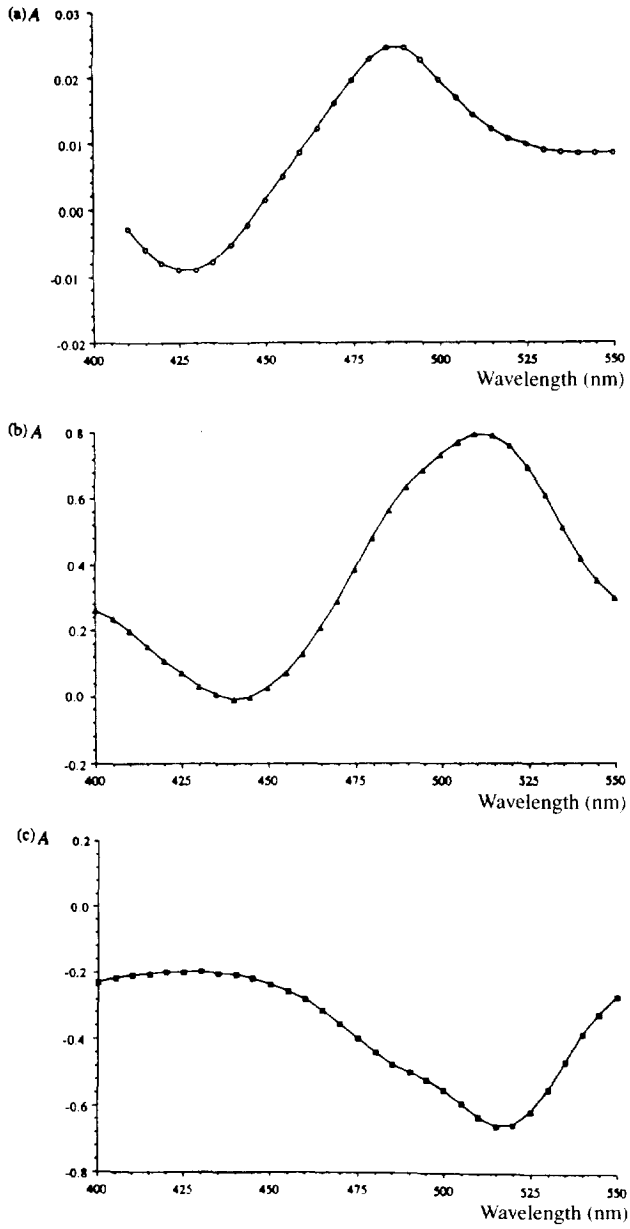

Fig 6. Successive difference absorption spectra of riboflavin/Moclobemide; (a) $(R/M)_0 - (R)_0$, (b) $(R/M)_{1D} - (R/M)_0$, (c) $(R/M)_{12D} - (RM)_{1D}$. $(R)_0$ = riboflavin just after solution formation, $(R/M)_0$ = riboflavin/Moclobemide just after solution formation, $(R/M)_{1D}$ = riboflavin/Moclobemide after 1 d of exposure to light, $(R/M)_{12D}$ = riboflavin/Moclobemide after 12 d of exposure to light; the scale of the different graphs is not identical for all plots.

reaction does not necessarily mimic the enzymatic reaction. Such extrapolations have been conclusive for Clorgyline and 1-Deprenyl but not for *N*-2-butynyl-*N*-methylbenzylamine and *N*-2,3-butadienyl-*N*-methylbenzylamine [28]. Consequently, as recommended by Muller [29] and Kim *et al* [30], we should avoid deducing the biological pertinence of an observed mechanism from a model photochemical study.

At this stage of the work, it is interesting to point out that Gates and Silverman have proposed that Moclobemide exerts its inhibitory activity by the same process as 5-(aminomethyl)-3-aryl-2-oxazolidinones and mechanism-based inhibitors [7]. This process involves a one-electron oxidation of the amine followed by α-proton removal simultaneous with the formation of a radical centred on the α carbon. After this, the so-formed radical combines with the other one within the active site.

In conclusion, Brofaromine, Harmine and R40519 form a charge-transfer complex with riboflavin in the same way as Toloxatone. In contrast, Moclobemide seems implicated in a succession of at least two molecular mechanisms. First, the formation of a charge-transfer complex and then the formation of a new chemical entity, which is unstable.

Ab initio Hartree–Fock quantum mechanical calculations

Beside the charge-transfer component, other bonding components such as electrostatic interactions and van der Waals forces also contribute to the stability of the different complexes. The relative contributions of these different bonding components between the MAO_AIs and riboflavin as well as the relative orientation of the two partners within the complex is governed by their electronic structure. Therefore, in order to explain the experimental results obtained by electronic absorption spectroscopy and to identify the different types of interactions which contribute to the stabilization of the riboflavin/Brofaromine, riboflavin/Harmine and riboflavin/R40519 complexes, several electronic parameters of Brofaromine, Harmine and R40519 were determined by quantum mechanical calculations; those of the flavin nucleus have been defined previously [10].

The wave functions associated with Brofaromine, Harmine and R40519 were computed at the *ab initio* STO-3G or STO-3G* Hartree–Fock level. Their analysis in terms of π overlap percentages, molecular electrostatic potentials and frontier orbital topologies allowed us to comprehend various features of the electronic distribution. First, the π overlap percentages, *ie* the ratios of the π overlap populations *versus* the total overlap populations (fig 7), give an idea of the delocalization schemes (fig 8) and the general electronic structures. Second, the molecular electrostatic potentials represent the interaction energy between a temporary positive charge and a non-disturbed distri-

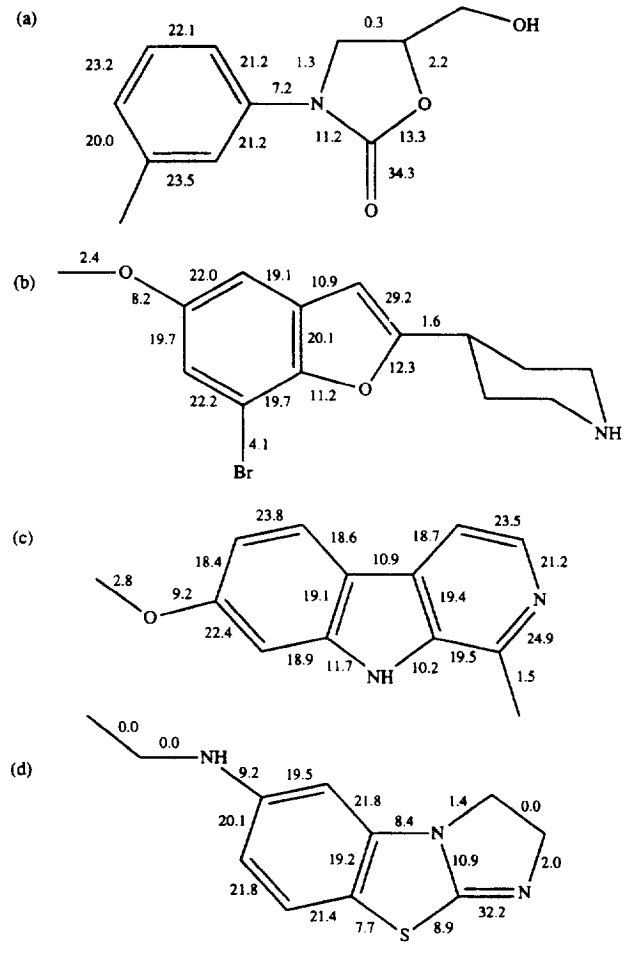

Fig 7. *Ab initio* HF STO-3G or STO-3G* π overlap percentages (%): (a) Toloxatone, (b) Brofaromine, (c) Harmine and (d) R40519.

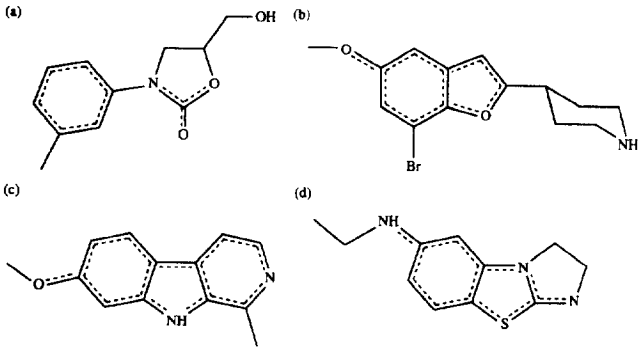

Fig 8. Delocalization scheme of (a) Toloxatone, (b) Brofaromine, (c) Harmine and (d) R40519.

bution of charges. Thus, the iso-contour maps of the molecular electrostatic potential at a distance close to the van der Waals radius (fig 9) supply a view of the electronic distribution as experienced by the approaching partner. The initial driving forces, as the ligand approaches the receptor site, are indeed mostly electrostatic. Finally, the analysis of the frontier orbital topologies of the interacting partners (fig 10) easily shows the presence or absence of charge-transfer interactions.

All four MAO_AIs, Brofaromine, Harmine, R40519 and Toloxatone, are characterized by at least two regions of high π-electron density: one formed within an aryl ring and another within a heterocyclic system, *ie* a furan (Brofaromine), a pyridine (Harmine), an imidazole (R40519) or an oxazolidinone (Toloxatone) (figs 7 and 8).

The iso-contour maps of the molecular electrostatic potential generated at 1.75 Å from the mean plane of the inhibitors show a large attractive zone (between −15 and −25 kcal mol^{-1}), whose minimum is located close to either the bromine of Brofaromine, the endocyclic nitrogen of Harmine and R40519, or the carbonyl of Toloxatone, and which extends over the aryl rings (fig 9). The profile of these maps can be considered as characteristic of the MAO_AIs.

Given the existence of charge transfer between riboflavin and the MAO_AIs, and given the well-established electron acceptor property of flavin compounds, the topologies of the highest occupied molecular orbital (HOMO) of the donors, *ie* the inhibitors, were analysed (fig 10). The HOMO of all the considered inhibitors are very similar. They are all π molecular orbitals clearly characterized by the $2p_\pi$ atomic orbitals as revealed by the highest and most dense electronic isodensity contours localized principally on the atoms of the aryl rings and on heteroatoms. The energies associated with these orbitals (table III) are correlated with the wavelength λ_{max} characteristic of the intermolecular transitions observed by electronic absorption (see previous section).

It should be noted that Moclobemide, which differs from other MAOIs in its biochemical and photochemical behaviour, is characterized by electronic properties that also differ from those of Toloxatone, Brofaromine, Harmine and R40519 [31].

Hypothetical interaction schemes with the FAD cofactor

Two major contributions to the stability of the complexes are electrostatic interactions and charge-transfer bonding. Electrostatic interactions are long-range forces that influence the approach of the MAO_AIs to the isoalloxazine ring and charge-transfer bonding is a short range force which occurs during the last step when the two partners are close to each other.

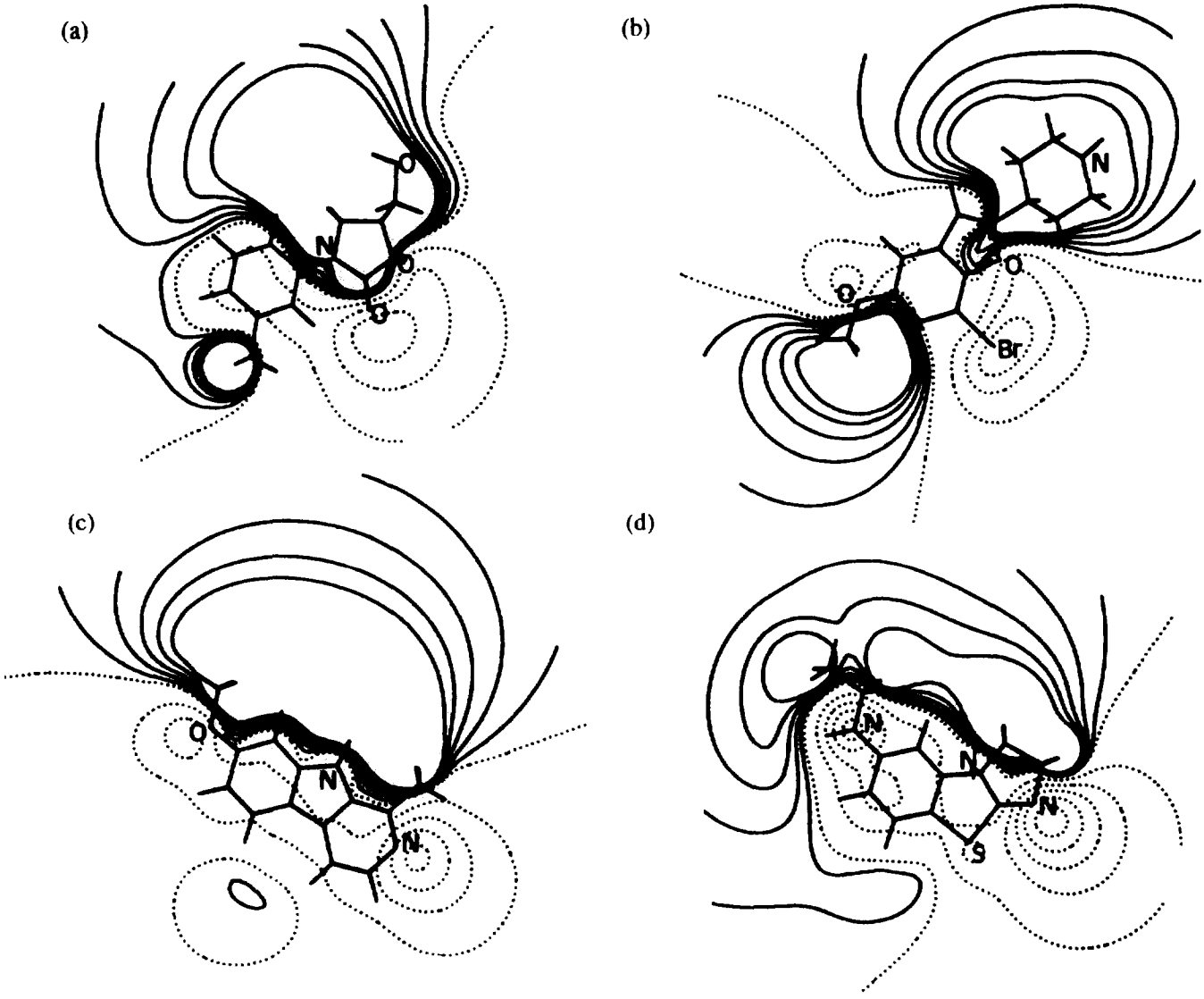

Fig 9. *Ab initio* HF STO-3G or STO-3G* iso-electrostatic potential energy maps (kcal mol^{-1}) (*XZ* plane at $Y = 1.75$ Å) for (a) Toloxatone, (b) Brofaromine, (c) Harmine and (d) R40519; attractive regions are represented by dotted lines, repulsive ones by solid lines; contour-to-contour intervals are 5 and 1 kcal mol^{-1}, respectively.

Taking these considerations into account, a hypothesis of interaction can be proposed for all inhibitors by superimposing them with the flavin cofactor on the basis of the molecular electrostatic potential maps and the frontier orbital topologies, as previously done for *R*-Toloxatone and the flavin nucleus [10].

First, each MAO_AI is orientated relative to the flavin nucleus so as to obtain the best complementarity between the repulsive and attractive zones of the two partners. The molecular electrostatic map of the flavin nucleus shows two large attractive zones induced by the carbonyls and a repulsive one which is spread over both sides of the tricyclic ring so as to form an inclusion between the two attractive zones [10]. On the other hand, all the MAO_AIs are characterized by a deep well of attractive potential, which is spread so as to cover the aryl ring.

This particular profile of the molecular electrostatic potential maps of MAO_AIs is quite complementary to that of the flavin nucleus (figs 11a, 12a and 13a).

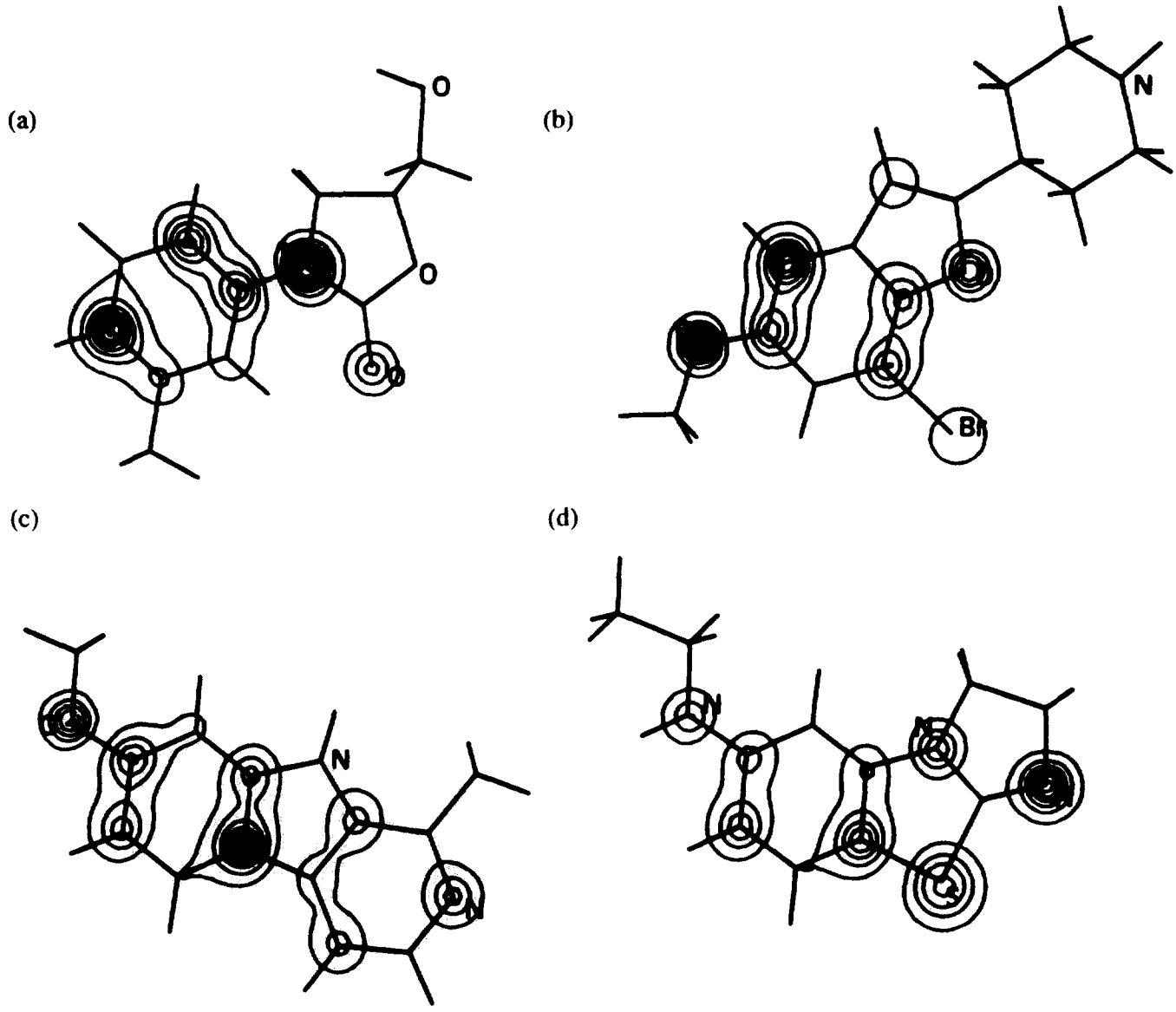

Fig 10. *Ab initio* HF STO-3G or STO-3G* iso-electron density maps ($e^-/Å^3$) of the highest occupied molecular orbital (HOMO) of (a) *R*-Toloxatone, (b) Brofaromine, (c) Harmine and (d) R40519; contour-to-contour interval is 10^{-2} $e^-/Å^3$.

Secondly, these preliminary hypotheses of interaction between the MAO_AIs and the flavin nucleus are further confirmed by the analysis of the frontier orbital topologies. Indeed, the orientations deduced from the potential maps allow a good overlap between the lowest unoccupied molecular orbital (LUMO) of the acceptor, *ie* the flavin nucleus, and the HOMO of the donors, *ie* the inhibitors. The charge transfers proposed from experimental measurements occur between the aryl rings and heteroatoms of MAO_AIs and the quinone-like heterocyclic part and the N_5 atom of the flavin nucleus (figs 11b, 12b and 13b).

Moreover, it is important to underline that the relative orientations of the partners deduced from these analyses allow not only electrostatic interactions and charge-transfer bonding but also maximum complementarity between van der Waals interactions. Indeed, all the high π electron density regions of the inhibitors are superimposed with the

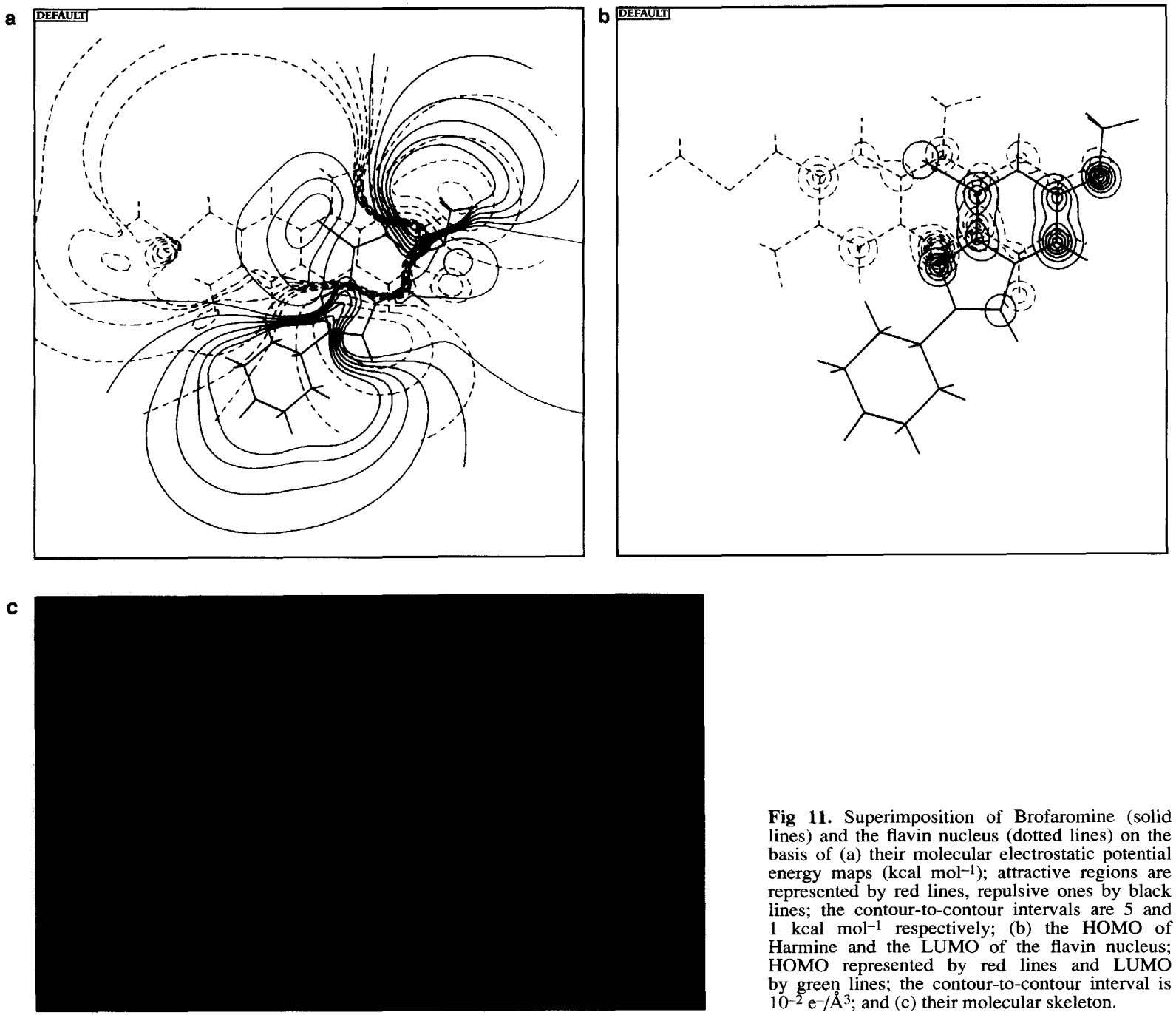

Fig 11. Superimposition of Brofaromine (solid lines) and the flavin nucleus (dotted lines) on the basis of (a) their molecular electrostatic potential energy maps (kcal mol^{-1}); attractive regions are represented by red lines, repulsive ones by black lines; the contour-to-contour intervals are 5 and 1 kcal mol^{-1} respectively; (b) the HOMO of Harmine and the LUMO of the flavin nucleus; HOMO represented by red lines and LUMO by green lines; the contour-to-contour interval is 10^{-2} $e^{-}/Å^3$; and (c) their molecular skeleton.

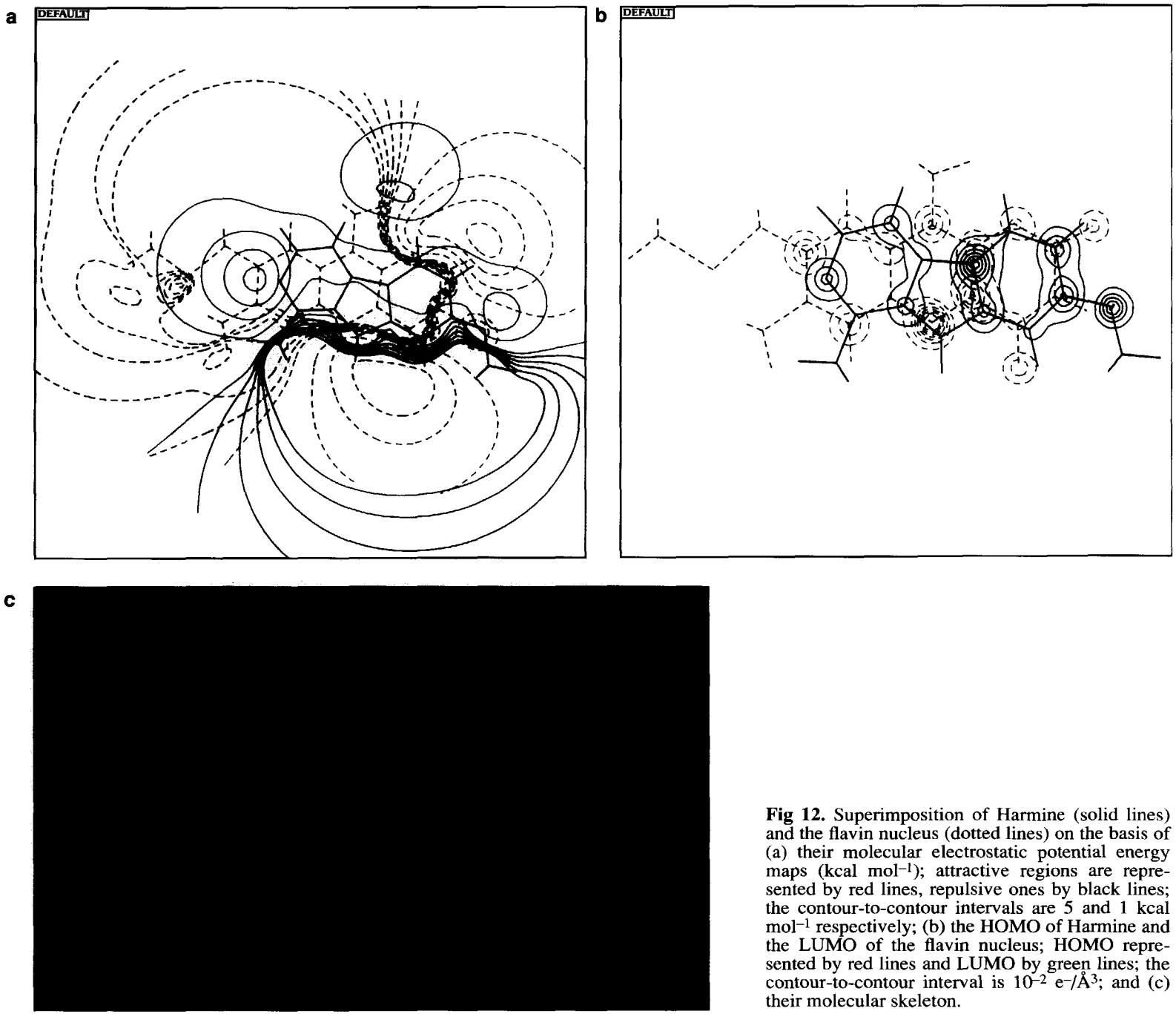

Fig 12. Superimposition of Harmine (solid lines) and the flavin nucleus (dotted lines) on the basis of (a) their molecular electrostatic potential energy maps (kcal mol^{-1}); attractive regions are represented by red lines, repulsive ones by black lines; the contour-to-contour intervals are 5 and 1 kcal mol^{-1} respectively; (b) the HOMO of Harmine and the LUMO of the flavin nucleus; HOMO represented by red lines and LUMO by green lines; the contour-to-contour interval is 10^{-2} $e^{-}/Å^3$; and (c) their molecular skeleton.

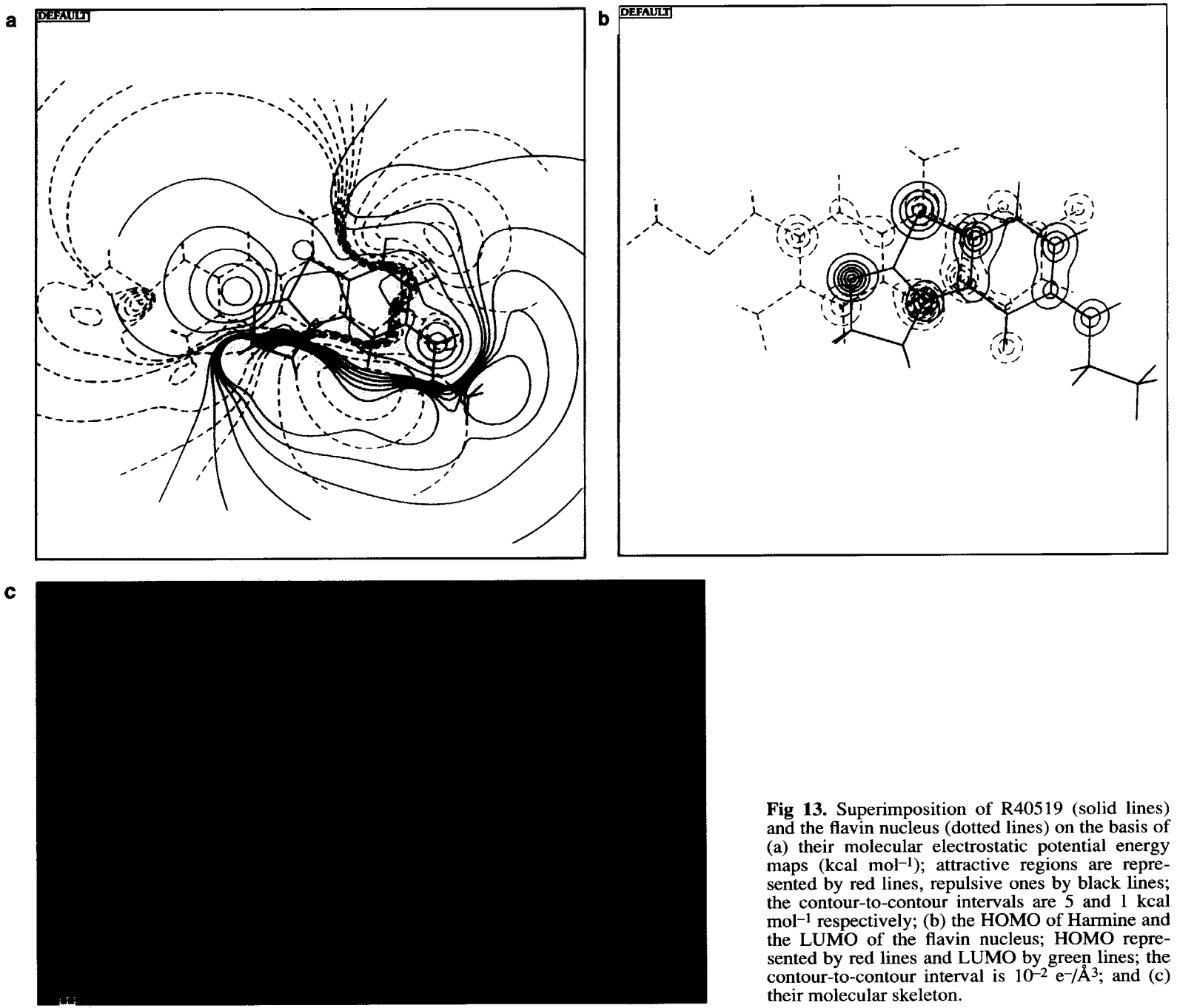

Fig 13. Superimposition of R40519 (solid lines) and the flavin nucleus (dotted lines) on the basis of (a) their molecular electrostatic potential energy maps (kcal mol^{-1}); attractive regions are represented by red lines, repulsive ones by black lines; the contour-to-contour intervals are 5 and 1 kcal mol^{-1} respectively; (b) the HOMO of Harmine and the LUMO of the flavin nucleus; HOMO represented by red lines and LUMO by green lines; the contour-to-contour interval is 10^{-2} $e^{-}/Å^3$; and (c) their molecular skeleton.

flavin nucleus which is characterized by a strongly delocalized structure [32] (fig 11c, 12c and 13c).

In conclusion, it is possible to orient Brofaromine, Harmine, R40519 relative to the flavin nucleus so as to obtain a good complementarity of the electronic descriptors of the different partners.

Conclusions

The essentially planar structure of most reversible inhibitors of MAO_A and the good aptitude of most of them to participate in π–π interactions [9] favoured the hypothesis according to which these compounds exert their inhibitory activity by weak and reversible interactions with FAD, the cofactor of the enzyme.

In order to verify the validity of such assumption, a sequence of experimental and theoretical studies was undertaken.

As shown by electronic absorption spectroscopy, in solution Brofaromine, Harmine, R40519 and *R*-Toloxatone [10] form a charge-transfer complex with riboflavin, a model of the flavin cofactor. However, Moclobemide seems to be implicated in a photochemical reaction.

The host/guest association in the complexes is stabilized by different types of bond: charge-transfer, electrostatic interactions and van der Waals forces. The contribution of these three different binding components and the relative orientation of the two partners within the complexes are both governed by the electronic structure, and so we compare the most important electronic descriptors of the MAO_AIs, as determined by the *ab initio* molecular orbital method.

Toloxatone, Brofaromine, Harmine and R40519 offer similar electronic profiles. First, they are all characterized by an electronically delocalized structure within an aromatic nucleus and a heterocycle. Second, and particularly for Toloxatone, Harmine and R40519, this aryl ring is covered by a zone of attractive potential at a distance close to the van der Waals radius and generated by the deeper attractive potential well of the molecule. Finally, their HOMOs are π-type orbitals, delocalized principally over the aryl ring and the heteroatoms.

All the described electronic properties of MAO_AIs are complementary to those of the flavin nucleus which was studied previously [10]. Consequently, by complementarity between the molecular electrostatic potential maps of the MAO_AIS and that of the flavin nucleus, and by superimposition of the frontier orbitals implicated in the charge-transfer bond, the HOMO of the MAO_AIs and the LUMO of the flavin nucleus, an interaction model similar to the one previously proposed for *R*-Toloxatone [10] can be defined for Brofaromine, Harmine, and R40519. In these four models, the aryl ring of the inhibitor is superimposed on the quinone-like ring of the flavin nucleus, and the attractive potential zone generated by the carbonyl of *R*-Toloxatone, the bromine of Brofaromine, the pyridinic nitrogen of Harmine and the imidazolic nitrogen of R40519 are in the same region, facing the aryl ring of the flavin nucleus (fig 14). Furthermore, the high π electron density zones of MAO_AIs are superimposed with the flavin nucleus, itself characterized by a strong electronic delocalization [32]. Thus, in addition to electrostatic interactions and charge transfers, this relative orientation of MAOIs and the flavin nucleus also favours van der Waals interactions between the two partners.

In conclusion, it is possible that the reversible MAO_A inhibitors, like the irreversible ones, exert their inhibitory activity by binding with the cofactor of the MAO_A. However, the nature of the binding involved is totally different. While irreversible MAO_AIs engage in covalent bonds with the flavin cofactor, reversible MAO_AIs interact by means of weak and labile forces. This is the case for four of the five reversible inhibitor studied; Moclobemide differs from the others because it is transformed by the flavin cofactor into a new reactive chemical entity after forming a reversible complex with the cofactor.

The proposition of an interaction model for MAO_AIs and the flavin moeity by comparison of their electronic descriptors constitutes an essential step towards the understanding of the mechanism of the inhibition at the molecular level. Confirmation of these hypotheses should be obtained by working with the entire MAO_A. This is currently under investigation.

Nevertheless this model seems useful for the design of new potent MAO_A inhibitors. Accordingly an aryloxazolidinone follow-up of Toloxatone has been identified, Befloxatone, which is in phase II clinical studies as an antidepressant [33].

Experimental protocols

Electronic absorption spectroscopy

The spectrophotometric measurements were carried out with an LKB Biochrom Ultrospec II 4050 spectrophotometer and a thermostatic cell holder. Constant temperature was maintained by circulating water. Glass cells of 1 cm pathlength were used. Products were dissolved in a phosphate buffer (pH = 6, ionic strength = 2×10^{-1} M). Concentrations of Brofaromine, Harmine, R40519 and Moclobemide ranged from 4.9×10^{-4} M to 1.3×10^{-2} M. The concentration of riboflavin was maintained constant and around 1.5×10^{-4} M. The temperature range was 9.5–44.6°C. Spectra were recorded with the LKB Wavelength Scan program.

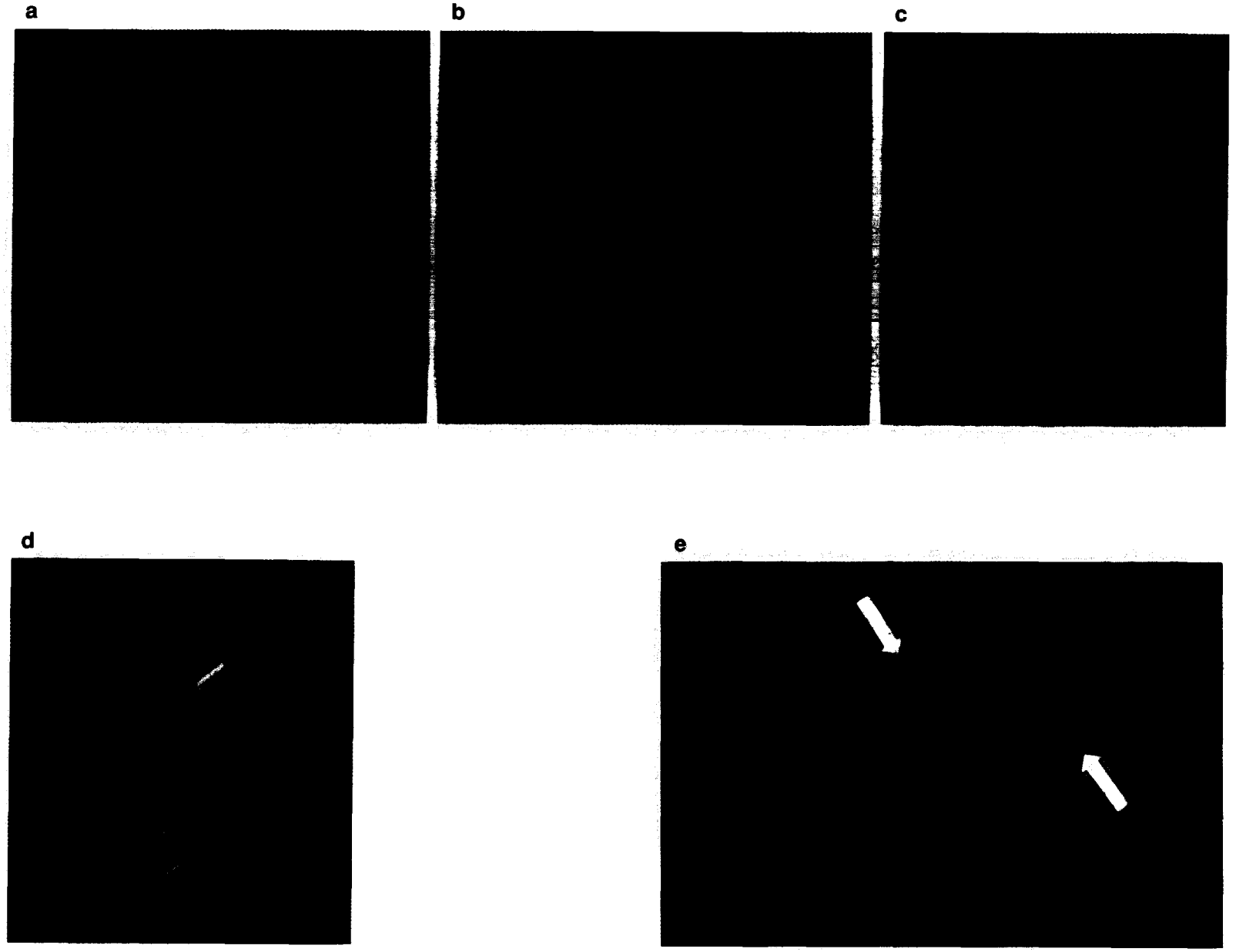

Fig 14. Interaction model between the flavin nucleus and (a) *R*-Toloxatone, (b) Brofaromine, (c) Harmine and (d) R40519, (e) molecular superimposition of all MAOIs and the flavin nucleus.

Ab initio Hartree–Fock calculations

Electronic properties were calculated using the RHF (restricted Hartree–Fock) LCAO-MO-SCF (linear combination of atomic orbitals–molecular orbital–self consistent field) electronic theory scheme [34]. The calculations were performed at two different degrees of sophistication of LCAO expansion of the molecular orbitals as introduced by Pople: STO-3G [35] for Harmine and STO-3G* [36] for Brofaromine and R40519 because of the presence of sulfur and bromine atoms. The bielectronic integral cut-off and convergence on the density matrix threshold were fixed at 10^{-8} au and 10^{-7}, respectively.

The internal coordinates of the heavy atoms considered in the calculation of Brofaromine, Harmine and R40519 were obtained from the crystallographic resolution [37–39]. The interatomic distances and valence angles of the hydrogen atoms were fixed at 1.084 or 1.090 Å and 120.0 or 109.471°, depending on the hybridization of the carrier atom, sp^2 and sp^3, respectively. The molecules were placed in the XZ plane in order to easily differentiate the π electron contribution (*ie* the $2p_y$ component) from the total contribution. All calculations were performed with the Gaussian 90 program [40].

The π overlap percentages, *ie* the ratio of π overlap population *versus* the total overlap population, were evaluated using the widely adopted Mulliken population analysis [41]. Molecular electrostatic potential values were calculated in planes at 1.75 Å from the mean plane of each molecule in the opposite side of the lateral chain according to the method of Scrocco and Tomasi [42, 43] (step between two grid points: 0.25 Å). The computation of the electron charge densities has been performed with the MOPLOT (Molecular Orbital Plot) program [44] available in the MOTECC library [45]. Our experience has shown that within the STO-3G, or STO-3G*, basis set the precision is *ca* 1 kcal mol^{-1} for the molecular orbital energy and 1–2 kcal mol^{-1} for electrostatic potential values.

Results obtained for *R*-Toloxatone and the flavin nucleus have been published previously [10]. All calculations were done on the IBM 9377/90 - FPS M64 computer system of the Scientific Computing Centre of the University of Namur.

Molecular graphics

Real-time interactive superimpositions of molecular models were done using IFMFIT (Improved or Interactive Flexible Molecular Fitting) [46, 47] implemented into KEMIT [48]. KEMIT is an in-house device-independent molecular graphics system developed in Fortran and using the IBM graPHICS software [45].

All 2D iso-contour maps and real-time interactive superimpositions of iso-contour maps were done using CMS-3D [49].

Acknowledgments

The authors thank the Belgian National Foundation for Scientific Research (FNRS), IBM-Belgium, and the Facultés Universitaires Notre-Dame-de-la-Paix for the use of the Namur Scientific Computing Facility (SCF) Center. JW acknowledges the FNRS for his Research Assistant position.

References

1 Greenwalt JW, Schnaitman C (1970) *J Cell Biol* 46, 173–179
2 Youdim MBH, Finberg JPM, Tipton KF (1988) *Handb Exp Pharmacol* 90, 119–192
3 Weyler W (1989) *Biochem J* 260, 725–729
4 Bach AWJ, Lan NC, Johnson DL *et al* (1988) *Proc Natl Acad Sci USA* 85, 4934–4938
5 Strolin Benedetti M, Dostert PL (1992) *Adv Drug Res* 23, 65–125
6 Silverman RB (1988) *In: Mechanism-Based Enzyme Inactivation: Chemistry and Enzymology*, CRC Press, Boca Raton, USA
7 Gates KS, Silverman RB (1990) *J Am Chem Soc* 112, 9364–9372
8 Dostert P, Strolin Benedetti M (1986) *Actual Chim Thér* 13, 269–287
9 Moureau F, Wouters J, Vercauteren DP *et al* (1992) *Eur J Med Chem* 27, 939–948
10 Moureau F, Wouters J, Vercauteren DP *et al* (1994) *Eur J Med Chem* 29, 269–277
11 Da Prada M, Kettler R, Keller HH, Burkard WP, Muggli-Maniglio D, Haefely WE (1989) *J Pharmacol Exp Ther* 248, 400–414
12 Anderson MC, Waldmeier PC, Tipton KF (1991) *Biochem Pharmacol* 41, 1871–1877
13 Moretti A, Caccia C, Galderini G, Menozzi M, Amico A (1981) *Biochem Pharmacol* 30, 2728–2731
14 Nelson DL, Herbet A, Petillot Y, Pichat L, Glowinski J, Hamon M (1979) *J Neurochem* 32, 1817–1827
15 McIsaac WM, Estevez V (1966) *Biochem Pharmacol* 15, 1625–1627
16 Ho BT, McIsaac WM, Walker KE, Estevez V (1968) *J Pharm Sci* 57, 269–274
17 van der Brempt C (1986) PhD Thesis, Facultés Universitaires Notre-Dame-de-la-Paix, Namur, Belgium
18 Da Prada M, Kettler R, Keller HH, Haefely WE (1983) *Mod Probl Pharmacopsychiatry* 19, 231–245
19 Burkard WP, Bonetti EP, Da Prada M *et al* (1989) *J Pharmacol Exp Ther* 248, 391–399
20 Fitton A, Faulds D, Goa KL (1992) *Drugs* 43, 561–596
21 Slifkin MA (1971) *In: Charge-Transfer Interactions of Biomolecules*. Academic Press, London, UK
22 Foster R (1969) *In: Organic Charge-Transfer Complexes*. Academic Press, London, UK
23 Foster R, Hammick DL, Wardley AA (1953) *J Chem Soc* IV, 3817–3820
24 Codoner A, Monzo IS, Tomas F, Valero R (1986) *Spectrochimica Acta* 42A, 765–769
25 Codoner A, Monzo IS, Medina P, Tomas F (1987) *Spectrochimica Acta* 43A, 389–394
26 Codoner A, Monzo IS, Tomas F, Valero R (1987) *Spectrochimica Acta* 43A, 1379–1384
27 Codoner A, Monzo IS, Ortiz C, Olba A (1989) *J Chem Soc Perkin Trans* 2, 107–111
28 Salach JI, Kenney WC, Nagy J, Peach C, Singer TP (1979) *Third Congress of the Hungarian Pharmacological Society*, Budapest, 73–84
29 Müller F (1983) *In: Radicals in Biochemistry vol 108* Springer, Berlin, Germany
30 Kim JM, Cho IS, Mariano PS (1991) *J Org Chem* 56, 4943–4955
31 Moureau F (1992) PhD Thesis, Facultés Universitaires Notre-Dame-de-la-Paix, Namur, Belgium
32 Wouters J, Moureau F, Perpète P, Norberg B, Evrard G, Durant F (1993) *J Cryst Spectrosc Res* (in press)
33 Koenig JJ, Moureau F, Vercauteren DP, Durant F, Ducrey F, Jarreau FX (1992) *Clin Pharmacol* 15, 424B
34 Pople JA (1977) *In: Application of Electronic Structure Theory* (Schaefer HF, ed) Modern Theoretical Chemistry, Plenum, New York, USA, 4, 95–170
35 Hehre WJ, Stewart RF, Pople JA (1969) *J Chem Phys* 51, 2657–2664
36 Collins JB, Schleyer PVR, Binkley JS, Pople JA (1976) *J Chem Phys* 64, 5142–5151
37 Sorée A (1984) BScThesis, Facultés Universitaires Notre-Dame-de-la-Paix, Namur, Belgium
38 van der Brempt C, Sorée A, Norberg B, Evrard G, Durant F (1985) *Bull Soc Chim Belg* 94, 159–160

39 van der Brempt C, Durant F, Evrard G (1986) *Bull Soc Chim Belg* 95, 139–140

40 Frisch MJ, Head-Gordon M, Trucks GW *et al* (1990) *'GAUSSIAN90 Revision H'*, Carnegie-Mellon Quantum Chemistry Publishing Unit, Pittsburgh, USA

41 Mulliken RS (1955) *J Chem Phys* 23, 1833–1840

42 Scrocco E, Tomasi J (1973) *In: Topics in Current Chemistry, New Concepts II*, 42 Springer-Verlag, New York, USA, 95–170

43 Scrocco E, Tomasi J (1978) *Adv Quantum Chem* 11, 115–193

44 Hinde RJ, Luken WL, Chin S (1988) *'MOPLOT'*, IBM Kingston Technical Report KGN-141, New York, USA

45 Chin S, Vercauteren DP, Luken WL *et al* (1989) *In: Modern Techniques in Computational Chemistry: MOTECC 89* (Clementi E, ed) ESCOM Publishers, Leiden, 499–546

46 Lejeune J, Michel AG, Vercauteren DP (1986) *J Mol Graphics* 4, 194–199

47 Lejeune J, Michel AG, Vercauteren DP (1986) *J Comp Chem* 7, 739–744

48 Vanderveken DJ, Vercauteren DP (1989) *KEMIT, a Molecular Graphics System, Rel 1.2*, Facultés Universitaires Notre-Dame-de-la-Paix, Namur, Belgium

49 Baudoux G, Dory M, Vercauteren DP (1993) *CMS3D, Contour Monitoring System for Three Dimensional Data, Rel 1*, Facultés Universitaires Notre-Dame-de-la-Paix, Namur, Belgium